J. Ocean Univ. China (Oceanic and Coastal Sea Research)
DOI 10.1007/s11802-015-2423-5
ISSN 1672-5182, 2015 14 (4): 636-644
http://www.ouc.edu.cn/xbywb/
E-mail:xbywb@ouc.edu.cn

Dynamic Positioning System Based on Active Disturbance Rejection Technology

LEI Zhengling, GUO Chen*, and FAN Yunsheng

Information Science and Technology College, *Dalian Maritime University*, *Dalian* 116026, *P. R. China*

(Received June 18, 2013; revised October 22, 2013; accepted June 3, 2015)

Abstract A dynamically positioned vessel, by the International Maritime Organization (IMO) and the certifying class societies (DNV, ABS, LR, *etc.*), is defined as a vessel that maintains its position and heading (fixed location or pre-determined track) exclusively by means of active thrusters. The development of control technology promotes the upgrading of dynamic positioning (DP) systems. Today there are two different DP systems solutions available on the market: DP system based on PID regulator and that based on model-based control. Both systems have limited disturbance rejection capability due to their design principle. In this paper, a new DP system solution is proposed based on Active Disturbance Rejection Control (ADRC) technology. This technology is composed of Tracking-Differentiator (TD), Extended State Observer (ESO) and Nonlinear Feedback Combination. On one hand, both TD and ESO can act as filters and can be used in place of conventional filters; on the other hand, the total disturbance of the system can be estimated and compensated by ESO, which therefore enhances the system's disturbance rejection capability. This technology's advantages over other methods lie in two aspects: 1) This method itself can not only achieve control objectives but also filter noisy measurements without other specialized filters; 2) This method offers a new useful approach to suppress the ocean disturbance. The simulation results demonstrate the effectiveness of the proposed method.

Key words DP; ADRC; TD; ESO; disturbance rejection

1 Introduction

The control technology has been undergoing a rapid development since the Industrial Revolution in both engineering and theoretical science fields, which stimulates different paradigms in control engineering. On one hand, engineers gain experience in the actual engineering practice by exploring control mechanisms, such as the proportional-integral-derivative (PID) type, which is called the industry paradigm (Gao, 2010), is a kind of typical control technology for passive disturbance rejection and reacts only when a system deviates from target. On the other hand, the control technology is a branch of applied mathematics and the control law is derived from mathematical models of the control process based on mathematical axioms and assumptions, where such a technology is called the modern control paradigm (Gao, 2006, 2010).

The development of the offshore dynamic positioning (DP) technology is no exception from the above two paradigms. In the 1960s the first DP system was introduced for horizontal modes of motion (surge, sway and yaw) using single-input/single-output PID control algorithms in combination with low-pass and/or notch filter (Asgeir, 2011). This is the first generation of DP systems. However, problems occurred in actual operations. Because of the passive disturbance rejection, the PID-controller-based system can only correct the existing deviations (Holvik, 1998) which may result in fatal losses, particularly for oil rigs. Besides, the phase lags of positioning error signal led by the adopted low pass filter may eventually ruin the positioning accuracy. In the 1970s more advanced output control methods based on multivariable optimal control and Kalman filter theory were proposed by Balchen *et al.* (1976). Based on Balchen *et al.*'s theory (1976), Kongsberg developed the second generation of DP systems Since the 1990s (Stein, 2009), several nonlinear DP controller designs have been proposed (Stephens *et al.*, 1995; Aarset *et al.*, 1998; Fossen and Grovlen, 1998; Bertin *et al.*, 2000; Agostinho *et al.*, 2009; Tannuri *et al.*, 2010; Volovodov *et al.*, 2007). Generally, all these designs belong to the model-based control system, for which a mathematical model is never a 100% accurate representation of a real vessel. However, by using the Kalman filtering technique, the model can be continuously corrected (Holvik, 1998). Even a mathematical vessel model is effectively updated by using the Kalman filter, the model-calculated disturbance can still not represent the real ocean disturbance, which will naturally lead to a limited disturbance rejection capability. Due to the complexity of ocean environment, to accurately model

* Corresponding author. Tel: 0086-411-84723720
E-mail: dmuguoc@126.com

the ocean disturbance is bound to be a difficult task. With the increasing demand for higher accuracy and reliability of the ship motion-control system, the better control technology with less dependence on mathematical models needs to be developed.

Gao (2006) proposed the necessity of a paradigm shift in the feedback control system design. The disturbance was estimated from the known input and output signals instead of attempting to model it. By compensating for the estimated disturbance, the system can be transformed to a chained-integrator plant that can be easily controlled. This is the core of the disturbance rejection paradigm, and the Active Disturbance Rejection Control (ADRC) technology (Han, 2009a) is a typical representation of this paradigm, which proposes an ingenious way to avoid the complex modeling of disturbances and provides an alternative for the solution of the dynamic positioning system.

In this paper, we will systematically analyze the positioning problem and propose a new solution for the dynamic positioning system under the disturbance rejection paradigm based on the ADRC. The problem formulation is given in Section 2. The DP system design solution is introduced in Section 3. Active disturbance rejection observer designs are discussed in Section 4. Simulations are developed in Section 5. Conclusion remarks are given in Section 6.

2 Problem Formulation

2.1 Problem Statement

One important control function of DP systems is the station-keeping (Strand, 1999). To maintain a fixed position, a ship is required not only to anchor at a specified location, but also to reject continuous disturbances caused by wind, waves and currents at the same time. These requirements lead to the following four problems: a) How is the ship position information obtained from the measured noisy signals? This is concerned with filtering. The accuracy of the acquired ship position information greatly affects the system's positioning capability. b) Which kind of control method can well perform positioning? c) Which kind of thruster allocation method can not only allocate optimum thrust to any propeller unit in use, but also minimize fuel consumption, wear and tear on the propulsion equipment? d) How does the ship resist ocean disturbances in real-time? These problems of the DP system are described in Fig.1. Using observers, one can measure low-frequency position, heading and speed. Based on the measurements, the DP controllers can be designed and the control outputs transformed to individual thruster command via the thruster allocation.

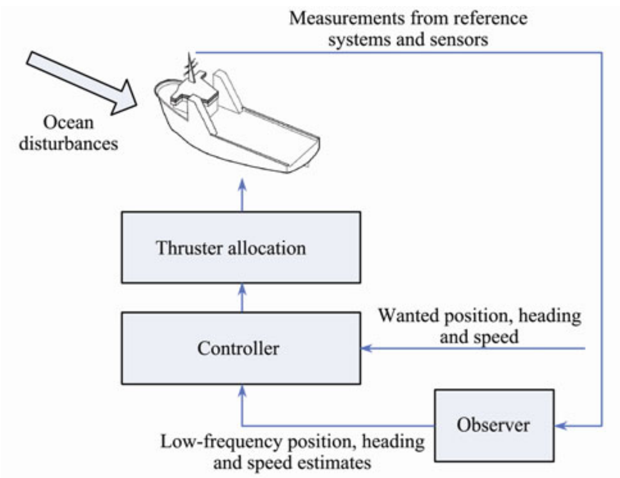

Fig.1 The description of problems in DP systems.

2.2 Vessel Model

The low-frequency (LF) motion of a large class of surface ships can be described in the body-fixed frame by the following model (Fossen, 1994):

$$\boldsymbol{M}\dot{\boldsymbol{v}} + \boldsymbol{C}(\boldsymbol{v})\boldsymbol{v} + \boldsymbol{D}(\boldsymbol{v} - \boldsymbol{v}_c) = \boldsymbol{\tau} + \boldsymbol{w}, \quad (1)$$

where, $\boldsymbol{v}=[u, v, r]^{\mathrm{T}}$ denotes the LF velocity vector, $\boldsymbol{v}_c=[u_c, v_c, r_c]^{\mathrm{T}}$ is the current vector, $\boldsymbol{\tau}=[\tau_1, \tau_2, \tau_3]^{\mathrm{T}}$ is the control force and moment vector, $\boldsymbol{w}=[w_1, w_2, w_3]^{\mathrm{T}}$ is the vector describing zero-mean Gaussian white noise processes. Note that $\boldsymbol{r}_c$ does not represent a physical current speed, but the effect of currents on the yaw of a ship.

The nonlinear damping forces can be neglected for dynamically positioned vessels if the linear hydrodynamic damping matrix $\boldsymbol{D}>0$ and the inertia matrix, including added mass terms, is assumed to be positive definite, $\boldsymbol{M}=\boldsymbol{M}^{\mathrm{T}}>0$. Assuming the symmetry of the starboard and the port, $\boldsymbol{M}$ and $\boldsymbol{D}$ can be written as:

$$\boldsymbol{M} = \begin{bmatrix} m - X_{\dot{u}} & 0 & 0 \\ 0 & m - Y_{\dot{v}} & mx_G - Y_{\dot{r}} \\ 0 & mx_G - Y_{\dot{r}} & I_z - N_{\dot{r}} \end{bmatrix}, \quad (2)$$

$$\boldsymbol{D} = \begin{bmatrix} -X_u & 0 & 0 \\ 0 & -Y_v & -Y_r \\ 0 & -Y_r & -N_r \end{bmatrix}, \quad (3)$$

here $\boldsymbol{M}=\{m_{ij}\}$ and, according to (2), the non-zero elements, $m_{ij}=-m_{ji}$, are defined as:

$$m_{11} = m - X_{\dot{u}},\ m_{23} = mx_G - Y_{\dot{r}},\ m_{22} = m - Y_{\dot{v}},\ m_{33} = I_z - N_{\dot{r}}.$$

The Coriolis and Centrifugal matrix $\boldsymbol{C}(\boldsymbol{v})$ is a function of the elements of the inertia matrix. Generally, $\boldsymbol{C}(\boldsymbol{v})$ can be expressed as:

$$\boldsymbol{C}(\boldsymbol{v}) = \begin{bmatrix} 0 & 0 & -m_{22}v - m_{23}r \\ 0 & 0 & m_{11}u \\ m_{22}v + m_{23}r & -m_{11}u & 0 \end{bmatrix}. \quad (4)$$

Most of the time $\boldsymbol{C}(\boldsymbol{v})=0$ for a ship; however, it may become significant when a ship is operating at certain speeds.

The kinematic equation of motion for a ship is:

$$\dot{\boldsymbol{\eta}} = \boldsymbol{J}(\boldsymbol{\eta})\boldsymbol{v} = \boldsymbol{R}(\psi)\boldsymbol{v}, \quad (5)$$

here $\boldsymbol{\eta}=[x, y, \psi]^{\mathrm{T}}$ denotes the position and orientation vector in the earth-fixed coordinate system, $\boldsymbol{v}=[u, v, r]^{\mathrm{T}}$ denotes the linear and angular velocity vector in the body-fixed coordinate system, and the rotation matrix $\boldsymbol{R}(\psi)$ is defined as:

$$\boldsymbol{R}(\psi)=\begin{bmatrix}\cos\psi & -\sin\psi & 0\\ \sin\psi & \cos\psi & 0\\ 0 & 0 & 1\end{bmatrix}.$$

The white noise dynamics and disturbances of the system can be described as (Fossen, 1994; Fossen and Strand, 1999):

$$\begin{cases}\boldsymbol{w}=\boldsymbol{J}^{\mathrm{T}}(\boldsymbol{\eta})\boldsymbol{b}\\ \dot{\boldsymbol{b}}=-\boldsymbol{T}_b^{-1}\boldsymbol{b}+\boldsymbol{E}_b\boldsymbol{\omega}_b\end{cases}, \quad (6)$$

here $\boldsymbol{b}\in\mathrm{R}^3$ is the vector of bias force and moment, $\boldsymbol{E}_b=\mathrm{diag}\{E_{b1}, E_{b2}, E_{b3}\}$, $\boldsymbol{\omega}_b$ represents the zero-mean Gaussian white noise, $\boldsymbol{T}_b$ is the diagonal matrix of positive bias time constants.

A linear wave frequency (WF) model of the order p can be generally expressed as (Fossen and Strand, 1999):

$$\dot{\xi}=\boldsymbol{\Omega}\xi+\Sigma\boldsymbol{\omega}_o, \quad (7)$$

$$\boldsymbol{\eta}_w=\boldsymbol{\Gamma}\xi, \quad (8)$$

where $\xi\in\mathrm{R}^{3*p}$, $\boldsymbol{\omega}_o\in\mathrm{R}^3$ and $\boldsymbol{\Omega}$, Σ and $\boldsymbol{\Gamma}$ are the constant matrices of appropriate dimensions. $\boldsymbol{\omega}_o$ is assumed to be the zero-mean Gaussian white noise.

A state-space description of the 2nd-order wave-induced motion in 3 degrees of freedom (DOF) (Sælid *et al.*, 1983) is:

$$\begin{bmatrix}\dot{\xi}_1\\ \dot{\xi}_2\end{bmatrix}=\begin{bmatrix}0 & \mathbf{I}\\ \boldsymbol{\Omega}_{21} & \boldsymbol{\Omega}_{22}\end{bmatrix}\begin{bmatrix}\xi_1\\ \xi_2\end{bmatrix}+\begin{bmatrix}0\\ \Sigma_2\end{bmatrix}\boldsymbol{\omega}_o, \quad (9)$$

$$\boldsymbol{\eta}_w=[0\ \mathbf{I}]\begin{bmatrix}\xi_1\\ \xi_2\end{bmatrix}, \quad (10)$$

where $\xi_1\in\mathrm{R}^3$, $\xi_2\in\mathrm{R}^3$ and:

$$\boldsymbol{\Omega}_{21}=-\mathrm{diag}\{\omega_1^2,\omega_2^2,\omega_3^2\},$$

$$\boldsymbol{\Omega}_{22}=-\mathrm{diag}\{2\zeta_1\omega_1, 2\zeta_2\omega_2, 2\zeta_3\omega_3\},$$

$$\Sigma_2=\mathrm{diag}\{\sigma_1,\sigma_2,\sigma_3\},$$

here $\boldsymbol{\omega}_i(i=1, 2, 3)$ is the dominant wave frequency, $\zeta_i(i=1, 2, 3)$ is the relative damping ratio and $\sigma_i(i=1, 2, 3)$ is the parameter related to the wave intensity.

Hence, the position and heading measurement model can be described as:

$$\boldsymbol{y}=\boldsymbol{\eta}+\boldsymbol{\eta}_w+\boldsymbol{w}_\eta, \quad (11)$$

where $\boldsymbol{\eta}_w$ is the vessel's WF motion due to the 1st-order wave-induced disturbance and $\boldsymbol{w}_\eta\in\mathrm{R}^3$ is the measured zero-mean Gaussian white noise.

Combining the above modeling processes yields the modeling system, and the structure diagram of the corresponding system (Fossen, 1994) is shown in Fig.2. The control command $\boldsymbol{u}$ is the sum of feedforward and feedback control actions. Generally speaking, the disturbances generated by ocean waves and currents are suppressed via the feedback control system while the wind is compensated by the feedforward control system. In some specific cases, currents are also settled in the feedforward loop.

$$\dot{\xi}=\boldsymbol{\Omega}\xi+\Sigma\boldsymbol{\omega}_o, \quad (12)$$

$$\dot{\boldsymbol{\eta}}=\boldsymbol{J}(\boldsymbol{\eta})\boldsymbol{v}, \quad (13)$$

$$\dot{\boldsymbol{b}}=-\boldsymbol{T}_b^{-1}\boldsymbol{b}+\boldsymbol{E}_b\boldsymbol{\omega}_b, \quad (14)$$

$$\boldsymbol{M}\dot{\boldsymbol{v}}=-\boldsymbol{C}(\boldsymbol{v})\boldsymbol{v}-\boldsymbol{D}(\boldsymbol{v}-\boldsymbol{v}_c)+\boldsymbol{J}^{\mathrm{T}}(\boldsymbol{\eta})\boldsymbol{b}+\boldsymbol{\tau}, \quad (15)$$

$$\boldsymbol{y}=\boldsymbol{\eta}+\boldsymbol{\eta}_w+\boldsymbol{w}_\eta. \quad (16)$$

2.3 Thruster Allocation Model

Assuming that $\boldsymbol{\tau}\in\mathrm{R}^3$ is the control vector of forces and moment, including the surge and sway forces as well as a yaw moment, $\boldsymbol{f}\in\mathrm{R}^n$ is the actuator command, and n is the number of thrusters, thus

$$\boldsymbol{\tau}=\boldsymbol{B}(\boldsymbol{\alpha})\boldsymbol{f}, \quad (17)$$

where,

$$\boldsymbol{B}(\alpha_i)=\begin{pmatrix}\cos\alpha_i\\ \sin\alpha_i\\ -y_i\cos\alpha_i+x_i\sin\alpha_i\end{pmatrix}. \quad (18)$$

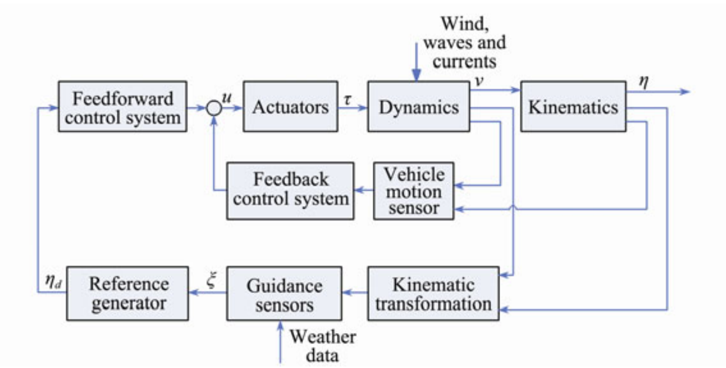

Fig.2 Guidance and control system for automatic ships.

In Eq. (18), α_i is the azimuth angle of the *i*-th thruster, and (x_i, y_i) are the coordinates of the *i*-th thruster.

The thruster allocation is not the focus of this paper, the thruster allocation model is developed according to Gu (2011). The constrained optimization problem for the azimuth $\boldsymbol{\alpha}$ is formulated as:

$$\min \boldsymbol{J}_{QP}(\Delta\boldsymbol{\alpha}, \Delta\boldsymbol{f}, \boldsymbol{s}) = \sum_{i=1}^{m}\left(\frac{\mathrm{d}W_i}{\mathrm{d}f_i}(f_{0,i})\Delta f_i + \frac{\mathrm{d}^2 W_i}{\mathrm{d}f_i^2}(f_{0,i})\Delta f_i^2\right) +$$

$$\boldsymbol{s}^{\mathrm{T}}\boldsymbol{Q}\boldsymbol{s} + \Delta\boldsymbol{\alpha}^{\mathrm{T}}\hat{\Omega}\Delta\boldsymbol{\alpha}\,, \tag{19}$$

which is subject to:

$$\boldsymbol{s} + \mathbf{B}(\boldsymbol{\alpha}_0)\Delta\boldsymbol{f} + \frac{\partial}{\partial\boldsymbol{\alpha}}(\mathbf{B}(\boldsymbol{\alpha})\boldsymbol{f})\big|_{f=f_0}^{\alpha=\alpha_0} \cdot\Delta\boldsymbol{\alpha} = \boldsymbol{\tau} - \mathbf{B}(\boldsymbol{\alpha}_0)\boldsymbol{f}_0\,,$$

$$\boldsymbol{f}_{\min}/p - \boldsymbol{f}_0 \le \Delta\boldsymbol{f} \le \boldsymbol{f}_{\max}/p - \boldsymbol{f}_0\,,$$

$$\Delta\boldsymbol{f}_{\min} \le \Delta\boldsymbol{f} \le \Delta\boldsymbol{f}_{\max}\,,$$

$$\boldsymbol{\alpha}_{\min} - \boldsymbol{\alpha}_0 \le \Delta\boldsymbol{\alpha} \le \boldsymbol{\alpha}_{\max} - \boldsymbol{\alpha}_0\,,$$

$$\Delta\boldsymbol{\alpha}_{\min} \le \Delta\boldsymbol{\alpha} \le \Delta\boldsymbol{\alpha}_{\max}\,,$$

where $W_i(f_i)=k_i|f_i|^{1.5}$ denotes the power consumption of individual actuator, and $k_i = \dfrac{2\pi K_q(0)}{D_1\sqrt{\rho K_t(0)^3}}$, K_t and K_q are the propeller thrust and the propeller torque coefficients, respectively. Azimuths $\boldsymbol{\alpha}_0$ and $\boldsymbol{f}_0$ are the optimal solutions from the previous sample; $\boldsymbol{f}_{\min}$ and $\boldsymbol{f}_{\max}$ are the lower and upper bounds of actuator command vectors; $\Delta\boldsymbol{f}_{\min}$ and $\Delta\boldsymbol{f}_{\max}$ are the lower and upper bounds of thrust vector variations; $\boldsymbol{\alpha}_{\min}$ and $\boldsymbol{\alpha}_{\max}$ are the lower and upper bounds of azimuth vectors; $\Delta\boldsymbol{\alpha}_{\min}$ and $\Delta\boldsymbol{\alpha}_{\max}$ are the lower and upper bounds of azimuth vector variations; $\boldsymbol{s}$ is the error between the anticipated and achieved general forces; $\Delta\boldsymbol{f}$ and $\Delta\boldsymbol{\alpha}$ are the variations of thrusts and azimuths, respectively. The large matrix $\boldsymbol{Q}>0$ is chosen so that the constraint (19) is satisfied with $\boldsymbol{s}\approx 0$ whenever possible. $\hat{\Omega} > 0$ is used to tune the objective function (19). Represented by the third term in (19), the rate-of-change in azimuths is constrained and minimized such that a large change is only allowed if it is necessary.

The constrained optimization problem for the thrust $\boldsymbol{f}$ is formulated as:

$$\min\{\boldsymbol{J} = \boldsymbol{f}^{\mathrm{T}}\boldsymbol{W}\boldsymbol{f} + \boldsymbol{s}^{\mathrm{T}}\boldsymbol{Q}\boldsymbol{s}\}\,, \tag{20}$$

which is subject to:

$$\boldsymbol{B}\boldsymbol{f} = \boldsymbol{\tau} + \boldsymbol{s}\,,\quad \boldsymbol{f}_{\min} \le \boldsymbol{f} \le \boldsymbol{f}_{\max}\,,\quad \Delta\boldsymbol{f}_{\min} \le \boldsymbol{f} - \boldsymbol{f}_0 \le \Delta\boldsymbol{f}_{\max}\,.$$

In this paper, the thrusts and their azimuths are calculated using quadratic programming (QP) methods and sequential quadratic programming (SQP) methods, respectively. The dynamic positioning system combining the vessel model and the thruster allocation model is established by using the Matlab stateflow toolbox (Guo and Lei, 2014).

3 DP System Solution Design Based on ADRC

3.1 Disturbance Rejection Paradigm

For this analysis, the ship motion model (13) and (15) can be rewritten as follows:

$$\ddot{\boldsymbol{\eta}} = \boldsymbol{f}(\boldsymbol{v}, \boldsymbol{\eta}, \boldsymbol{v}_c, \boldsymbol{b}) + \hat{\boldsymbol{U}}\,, \tag{21}$$

where

$$\boldsymbol{f}(\boldsymbol{v}, \boldsymbol{\eta}, \boldsymbol{v}_c, \boldsymbol{b}) = \boldsymbol{J}(\boldsymbol{\eta})\mathbf{M}^{-1}(-\boldsymbol{C}(\boldsymbol{v})\boldsymbol{v} - \boldsymbol{D}(\boldsymbol{v} - \boldsymbol{v}_c) + \boldsymbol{J}^{\mathrm{T}}(\boldsymbol{\eta})\boldsymbol{b}) + \dot{\boldsymbol{J}}(\boldsymbol{\eta})\boldsymbol{v}$$

and $\hat{\boldsymbol{U}} = \boldsymbol{J}(\boldsymbol{\eta})\boldsymbol{M}^{-1}\boldsymbol{\tau}$ is the introduced virtual control.

Generally speaking, the system uncertainties are known as the 'internal disturbance' while the outside perturbations are the 'external disturbance'. In the ship dynamic positioning system (21), the 'internal disturbance' and the 'external disturbance' are jointly expressed as $\boldsymbol{f}(\boldsymbol{v}, \boldsymbol{\eta}, \boldsymbol{v}_c, \boldsymbol{b})$, which is partially known in most situations.

In the disturbance rejection paradigm, the total disturbance is estimated in real time from the input and output signals, $\boldsymbol{f}\approx\boldsymbol{f}(\boldsymbol{v}, \boldsymbol{\eta}, \boldsymbol{v}_c, \boldsymbol{b})$. Thus, (21) can be transformed to

$$\ddot{\boldsymbol{\eta}} = \boldsymbol{u}_0\,, \tag{22}$$

through

$$\hat{\boldsymbol{U}} = -\hat{\boldsymbol{f}} + \boldsymbol{u}_0\,. \tag{23}$$

Therefore

$$\boldsymbol{\tau} = \boldsymbol{M}\boldsymbol{J}^{-1}(\boldsymbol{\eta})(-\hat{\boldsymbol{f}} + \boldsymbol{u}_0)\,, \tag{24}$$

where Formula (22) is a chained-integrator system that can be coped with a simple PD controller.

The key issue under this paradigm, also the core of active disturbance rejection control principle, is about how to estimate the total disturbance $\boldsymbol{f}(\boldsymbol{v}, \boldsymbol{\eta}, \boldsymbol{v}_c, \boldsymbol{b})$. There are three important parts in ADRC, namely Tracking-Differentiator (TD), Extended State Observer (ESO) and Nonlinear Feedback Combination (Han, 2009b). The ADR control framework is given in Fig.3. The disturbance Z_3 is estimated in the closed loop, which reduces the system to a chained-integrator plant.

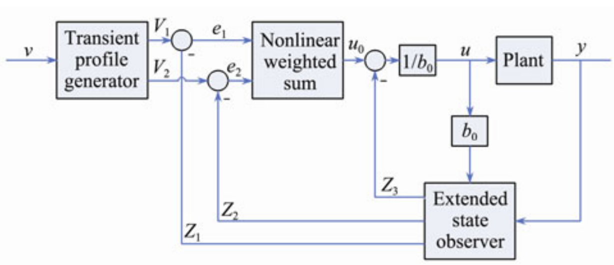

Fig.3 ADR control framework.

1) Tracking-differentiator

A TD introduced in the system is to obtain the fastest tracking and the derivative of the setpoint η_i^*. A brief introduction of TD design is given as follows:

$$\begin{cases} \dot{v}_1 = v_2 \\ \dot{v}_2 = \text{fhan}(v_1, v_2, u, r, h) \end{cases}, \tag{25}$$

where r is a parameter controling the tracking speed while h decides the filtering effect when the input signal is polluted by noise. The function fhan is calculated as follows:

$$\delta = rh, \quad \delta_0 = \delta h, \quad y = v_1 - u + hv_2, \quad a_0 = \sqrt{\delta^2 + 8r|y|},$$

$$a = \begin{cases} v_2 + y/h, |y| \le \delta_0 \\ v_2 + 0.5(a_0 - \delta)\text{sign}(y), |y| > \delta_0 \end{cases},$$

$$\text{fhan} = \begin{cases} -ra/\delta, |a| \le \delta \\ -r\,\text{sign}(a), |a| > \delta \end{cases}. \tag{26}$$

The weak convergence of non-linear high-gain tracking differentiator can be referred to Guo and Zhao (2013). By properly selecting r and h, η_i^* can be tracked very well and a smooth derivative of η_i^* can be obtained.

2) Nonlinear feedback combination

A nonlinear PD controller, chosen as the nonlinear feedback combination in this study, is depicted as follows:

$$\begin{cases} e_1 = \eta_i^* - \eta_i \\ e_2 = \dot{\eta}_i^* - \dot{\eta}_i \\ u_0 = \beta_1\,\text{fal}(e_1, a_1, \delta) + \beta_2\,\text{fal}(e_2, a_2, \delta) \end{cases}, \tag{27}$$

where

$$\text{fal}(e, a, \delta) = \begin{cases} e\delta^{a-1}, |e| \le \delta \\ |e|^a\,\text{sign}(e), |e| > \delta \end{cases}. \tag{28}$$

Combined with Formula (23), the virtual control is

$$\hat{U}_i = -\hat{f}_i + \beta_{1i}\,\text{fal}(e_1, a_1, \delta) + \beta_{2i}\,\text{fal}(e_2, a_2, \delta). \tag{29}$$

By using an ESO, $\hat{f}_i$ can be obtained from Eq. (30), which forms the core problem of disturbance rejection paradigm.

3) Extended State Observer

The mathematical description of the ESO is given as follows:

$$\begin{cases} E_1 = Z_1 - \eta_i \\ \dot{Z}_1 = Z_2 - \beta_3 E_1 \\ \dot{Z}_2 = Z_3 - \beta_4\,\text{fal}(E_1, a_3, \delta) + U_i \\ \dot{Z}_3 = -\beta_5\,\text{fal}(E_1, a_4, \delta) \end{cases}, \tag{30}$$

where E_1 is the estimation error of the NLESO, Z_1, Z_2 and Z_3 are the observer output, and β_3, β_4, and β_5 are the observer gains. For properly selected values of β_3, β_4, and β_5, Z_1, Z_2 and Z_3 approach η_i, $\dot{\eta}_i$, and $f_i(\boldsymbol{v}, \boldsymbol{\eta}, \boldsymbol{v}_c, \boldsymbol{b})$, respectively. Han (2009a) suggested that $\beta_3 = \frac{1}{h}, \beta_4 = \frac{1}{3h^2}$, and $\beta_5 = \frac{2}{8^2 h^3}$ for parameter tuning, where h is the sampling step. However, it can present questions in engineering practice. Further investigation of the non-linear ESO convergence for a class of non-linear multi-input/-output systems can be referred to Guo and Zhao (2012).

The control objectives can be achieved by properly selecting the values of β_1, β_2, β_3, β_4, β_5, a_3, a_4, and δ.

3.2 ADRC Based Solution for DP Systems

The ADRC based solution for the problem presented in 2.1 is discussed in this section. Some researchers found the good filtering characteristics of both TD and ESO (Song *et al.*, 2003; Zhu *et al.*, 2006; Wu *et al.*, 2004). Apart from that, ESO can be used to estimate and compensate for, in real time, the combined effects of the ‘internal disturbance’ and ‘external disturbance’, forcing an otherwise unknown plant to behave like a nominal one (Zheng and Gao, 2010). Therefore, based on ADRC, the filtering problem a) can be solved by TD, and the control problem b) and disturbance rejection problem d) can be settled by a combination of ESO and nonlinear feedback. Together with an optimization approach in thruster allocation, the solution can be described in Fig.4.

Remark 1: The solution in Fig.4 is given based on the assumption that a speed vector is measurable. When the speed vector is unmeasurable, the solution can be given by using the position and heading measurements in place of speed measurements as ESO input, which is consistent with the problem description by Eqs. (21)–(23).

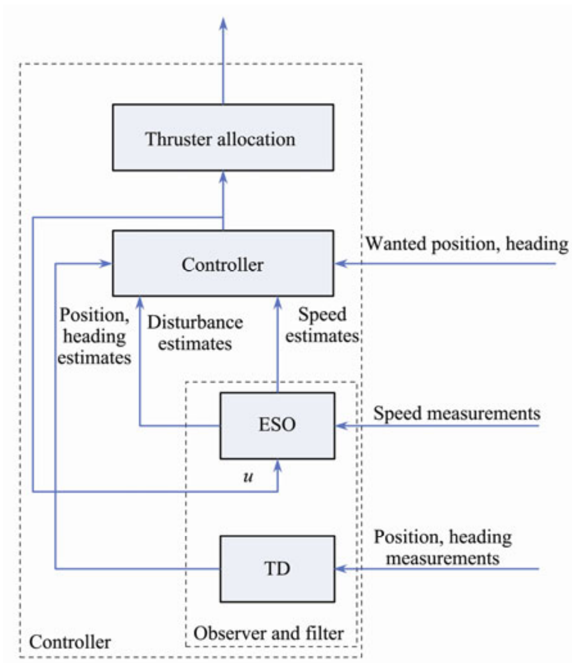

Fig.4 ADRC based solution for DP systems.

4 Active Disturbance Rejection Observer for DP Systems

4.1 Why are Observers Important for DP Systems?

It is known that only slowly-varying disturbances should be counteracted by a propulsion system, while wave-induced oscillatory motion should not enter the feedback loop (Fossen and Strand, 1999). Unfortunately, the position and heading measurements are contaminated by colored noises due to wind, waves and ocean currents as well as sensor noise. Without filtering out the noises damage to thrusters may result.

A scaled replica of the offshore supply vessel named CS2 was built and tested as the control plant for the study (Karl-Petter, 2003). The model has an overall length of L_{OA}=1.255 m, and is equipped with three propulsive devices: a small two-bladed RPM-controlled tunnel-thruster in the bow, producing a sway force, and two RPM-controlled main propellers with rudders at the stern. The specific coordinates of the three thrusters are as follows:

$$r_1 = (l_{1,x}, l_{1,y})^{\mathrm{T}} = (-0.054, -0.075),$$

$$r_2 = (l_{2,x}, l_{2,y})^{\mathrm{T}} = (-0.054, 0.075),$$

$$r_3 = (l_{3,x}, l_{3,y})^{\mathrm{T}} = (1.14, 0, 0),$$

where r_1, r_2 and r_3 represent the coordinates of the left and right stern thruster and the tunnel-thruster in the bow, respectively (Karl-Petter, 2003).

In the simulations the control inputs were set as:

$$\boldsymbol{\tau} = \begin{bmatrix} \sin(0.05t) \\ \sin(0.1t) \\ \sin(0.07t) \end{bmatrix}. \quad (31)$$

The measured noises were set as a vector of the zero-mean Gaussian white noise, and the variances were set as 1. The thruster system obtained data from the control outputs at a one-second sampling interval. The speed information was acquired from the position and heading measurements via TD, instead of the speed measurements. The thrusts and azimuths of the three thrusters were obtained by using the optimization method proposed in Section 2.3, and the corresponding results are shown in Fig.5.

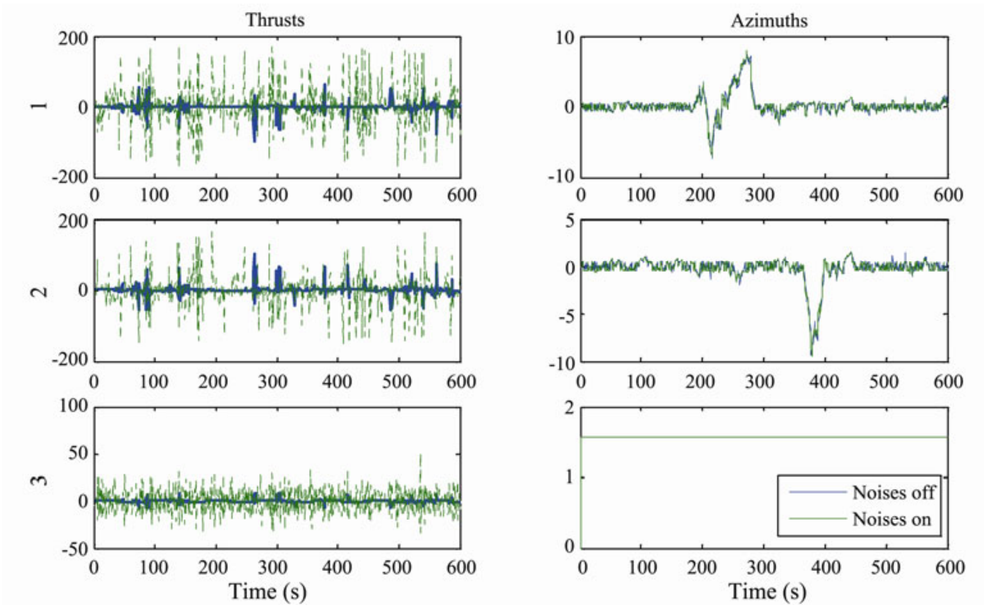

Fig.5 Thrusts and azimuths of the three thrusters.

Comparing to the results without measurement noise, it can be seen that the noise entering the propulsion system would lead to high frequency oscillations on all three thrusters, and therefore severely damage propellers. The wave filtering technique can be used to avoid the potential propeller damage by separating the position and heading measurements into a low-frequency (LF) and a wave frequency (WF) signal (Fossen, 1994).

In order to obtain the estimation of the ship position, heading and speed by ADRC, the system model, Eqs. (12)–(16), can be rewritten as two subsystems:

$$\text{(a)} \quad \begin{cases} \boldsymbol{M}\dot{\boldsymbol{v}} = -\boldsymbol{C}(\boldsymbol{v})\boldsymbol{v} - \boldsymbol{D}(\boldsymbol{v}-\boldsymbol{v}_c) + \boldsymbol{J}^{\mathrm{T}}(\boldsymbol{\eta})\boldsymbol{b} + \boldsymbol{\tau} \\ \boldsymbol{y}_v = \boldsymbol{v} + \boldsymbol{v}_w + \boldsymbol{w}_v \end{cases}, \quad (32)$$

$$\text{(b)} \quad \begin{cases} \dot{\boldsymbol{\eta}} = \boldsymbol{J}(\boldsymbol{\eta})\boldsymbol{v} \\ \boldsymbol{y}_\eta = \boldsymbol{\eta} + \boldsymbol{\eta}_w + \boldsymbol{w}_\eta \end{cases}, \quad (33)$$

where $\dot{\boldsymbol{\xi}} = \boldsymbol{\Omega}\boldsymbol{\xi} + \sum \boldsymbol{\omega}_o$, $\dot{\boldsymbol{b}} = -\boldsymbol{T}_b^{-1}\boldsymbol{b} + \mathbf{E}_b\boldsymbol{\omega}_b$. $\boldsymbol{v}_{\mathrm{w}}$ and $\boldsymbol{\eta}_w$ are the 1st-order wave-induced speed and motion, respectively, and $\boldsymbol{w}_v$ and $\boldsymbol{w}_\eta$ are the zero-mean Gaussian white noises. The speed estimates can be obtained by ESO based on system (a), while the position and heading estimates can be acquired by TD based on system (b).

4.2 Observers' Design

The ESO applied here are described as:

$$\begin{cases} E_0 = Z_1 - v_i \\ \dot{Z}_1 = Z_2 - \beta_6 E_0 + \hat{U}_i \\ \dot{Z}_2 = -\beta_7 \,\mathrm{fal}(E_0, a_5, \delta) \end{cases}. \quad (34)$$

With properly assigned β_6, β_7, and a_5, Z_1 can approach the LF speed and Z_2 approaches the total disturbance exerting on system (a). A TD defined by Eq. (25) can act as a filter here to present the LF position and heading estimates from the noisy measurements.

5 Simulation Study

5.1 Active Disturbance Rejection Observer Validation

The total disturbance and noise of DP systems consist of the following components:

1) External slowly-varying disturbances caused by wind, waves and currents;

2) Uncertainties;

3) Noises generated from vehicle motion sensors and 1st-order waves;

4) Noises generated from guidance sensors and 1st-order waves.

All the above disturbances should be rejected and suppressed by the ADRC. Fig.2 shows how the disturbances affect the system.

The simulation studies were conducted by the following settings:

1) In slowly-varying disturbance model (14), $\boldsymbol{T}_b$=diag{1000, 1000, 1000}, $\boldsymbol{E}_b$=diag{1, 1, 1}, the variance of $\boldsymbol{\omega}_b$ is 0.01.

2) In the 1st-order wave-induced noise model (12), $\omega_1=\omega_2=\omega_3=2$, $\zeta_1=\zeta_2=\zeta_3=0.2$, $\sigma_1=\sigma_2=\sigma_3=1$, $\boldsymbol{\Gamma}=[0\ \boldsymbol{I}]$. The variances of the zero-mean Gaussian white noise in $\boldsymbol{v}_w$ and $\boldsymbol{\eta}_w$ are 0.1 and 10000, respectively.

3) In the noise model generated from vehicle motion sensors, the variance of $\boldsymbol{w}_v$ is 0.1.

4) In the noise model generated from guidance sensors, the variance of $\boldsymbol{w}_\eta$ is 10.

5) The control inputs are chosen as (31).

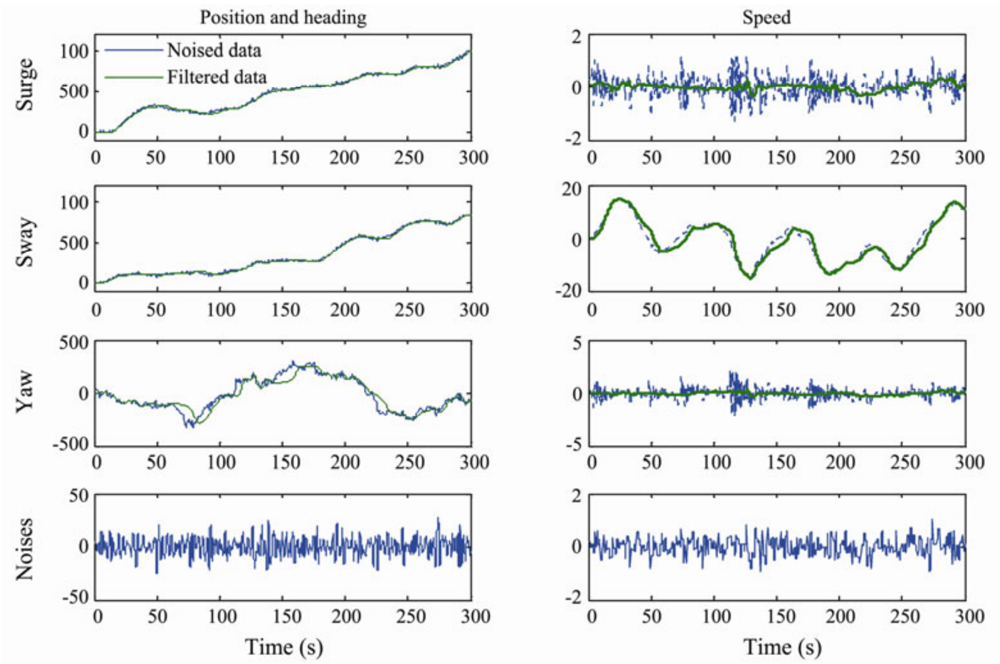

Fig.6 Calculated ship position, heading, and speed.

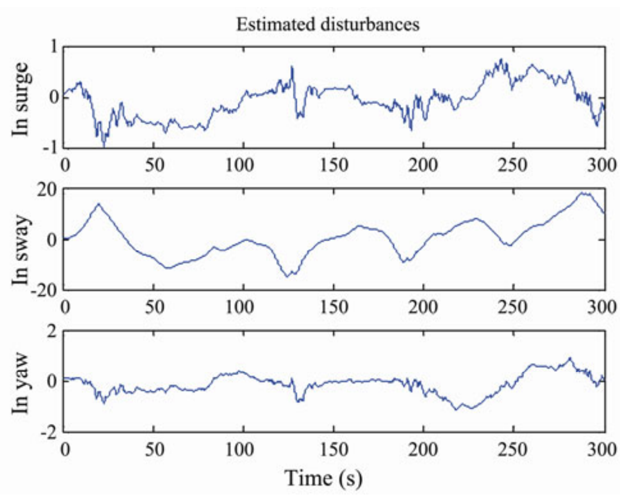

Fig.7 Estimation of total disturbances in surge, sway and yaw.

According to the ADRC based solution for DP systems in Fig.4, the position and heading estimates were acquired via TD, while speed and disturbance estimates by ESO. Fig.6 shows the calculated ship position, heading, and speed, and Fig.7 shows the total disturbance of the system. The curves demonstrate the filtering capability of proposed ADR observers, which also raises a question about whether ESO or TD possesses better filtering capability. Seeking answers to this question may lead to promising future research.

5.2 Validation of Active Disturbance Rejection Controller

With the ADRC applied to DP systems, even all the above described disturbances are exerted on the ship, the simulation results Fig.8 reveal that the ship can precisely sail towards the targeted location over the shortest path, exhibiting good positioning performance and disturbance rejection.

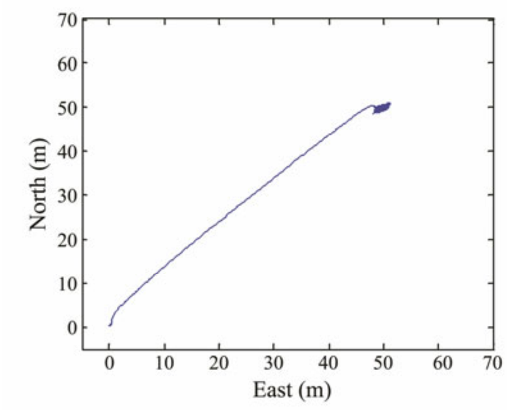

Fig.8 Ship position response curve of ADRC system.

6 Conclusions

A good DP system should solve the two key problems of noise filtering and disturbance rejection, while performing highly accurate positioning. An active disturbance rejection based technology tackles the two issues from a new perspective. On one hand, it eliminates the need for accurate modeling, estimates, and compensates for both the 'internal disturbance' and 'external disturbance' of the system via an extended state observer; the simulation results of the proposed DP method demonstrate its disturbance rejection capability. On the other hand, both the ESO and TD show good filtering characteristics, which can be used as an alternative filter for DP system solutions. However, the method is still in its primitive form of ADRC. A new ADRC solution custom-made for offshore dynamic positioning needs to be explored in the future.

Acknowledgements

The authors would like to thank the editor and anonymous reviewers for their careful reading and valuable suggestions. The support of the National Nature Science Foundation of China (Nos. 61074053 and 61374114) and the Applied Basic Research Program of Ministry of Transport of China (No. 2011-329-225-390) are gratefully acknowledged.

References

Aarset, M. F., Strand, J. P., and Fossen, T. I., 1998. Nonlinear vectorial observer backstepping with integral action and wave filtering for ships. *Proceedings of the IFAC Conference on Control Applications in Marine Systems*. Fukuoka, Japan, 83-89.

Agostinho, A. C., Moratelli Jr., I., Tannuri, E. A., and Morishita, H. M., 2009. Sliding mode control applied to offshore dynamic positioning systems. *Proceedings of the IFAC International Conference on Manoeuvring*. Guarujá, Brazil, 237-242.

Asgeir, J. S., 2011. A survey of dynamic positioning control systems. *Annual Reviews in Control*, **35** (1): 123-136.

Balchen, J. G., Jenssen, N. A., and Sælid, S., 1976. Dynamic positioning using kalman filtering and optimal control theory. *IFAC/IFIP Symposium on Automation in Offshore Oil Field Operation*. Amsterdam, The Netherlands, 183-186.

Bertin, D., Bittanti, S., Meroni, S., and Savaresi, S. M., 2000. Dynamic positioning of a single-thruster vessel by feedback linearization. *Proceedings of the IFAC Conference on Manoeuvring and Control of Marine Craft*. Aalborg, Denmark.

Fossen, T. I., 1994. *Guidance and Control of Ocean Vehicles*. John Wiley & Sons Inc., NewYork, 18-56.

Fossen, T. I., and Grovlen, A., 1998. Nonlinear output feedback control of dynamically positioned ships using vectorial observer backstepping. *IEEE Transactions on Control Systems Technology*, **6** (1): 121-128.

Fossen, T. I., and Strand, J. P., 1999. Passive nonlinear observer design for ships using Lyapunov Methods: Full-scale experiments with a supply vessel. *Automatica*, **35** (1): 3-16.

Gao, Z., 2006. Active disturbance rejection control: A paradigm shift in feedback control system design. *Proceedings of the 2006 Anerican Control Conference*. Minneapolis, Minnesota, USA, 2399-2405.

Gao, Z., 2010. On disturbance rejection paradigm in control engineering. *Proceedings of the 29th Chinese Control Conference*. Beijing, China, 6071-6076 (in Chinese).

Gu, L., 2011. Study on simulation technology of ship dynamic positioning system. Master thesis. China Ship Research Institute (in Chinese).

Guo, B. Z., and Zhao, Z. L., 2012. On convergence of non- linear extended state observer for multi-input multi-output systems with uncertainty. *IET Control Theory and Applications*, **6** (15): 2375-2386.

Guo, B. Z., and Zhao, Z. L., 2013. Weak convergence of nonlinear high-gain tracking differentiator. *IEEE TRAnsactions On AUtomatic Control*, **58** (4): 1074-1080.

Guo, C., and Lei, Z., 2014. Study on modeling and simulation for marine dynamic positioning hierarchical control system. *Journal of System Simulation*, **26** (5): 1118-1124 (in Chinese).

Han, J., 2009a. *Active Disturbance Rejection Control Technique–The Technique for Estimating and Compensating the Uncertainties*. National Defense Industry Press, Beijing, 243-280 (in Chinese).

Han, J., 2009b. From PID to active disturbance rejection control. *IEEE Transactions on Industrial Electronics*, **56** (3): 900-906.

Holvik, J., 1998. Basics of dynamic positioning. *Dynamic Positioning Conference*. Houston, 1-9.

Karl-Petter, W. L., 2003. Acceleration feedback in dynamic positioning. PhD thesis. Norwegian University of Science and Technology.

Lei, Z. L., Guo, C., and Liu, Y., 2012. Ship dynamic positioning decoupling control based on ADRC. *Proceedings of the 2012 International Conference on Intelligent Systems and Knowledge Engineering*, Beijing, 443-455.

Sælid, S., Jenssen, N. A., and Balchen, J. G., 1983. Design and analysis of a dynamic positioning system based on Kalman Filtering and optimal control. *IEEE Transactions on Automatic Control*, TAC-**28** (3): 331-339.

Song, J. L., Gan, Z. X., and Han, J. Q., 2003. Study of active disturbance rejection controller on filtering. *Control and Decision*, **18** (1): 110-112 (in Chinese).

Stein, B., 2009. Shipshaped: Kongsberg industry and innovations in deepwater technology, 1975–2007. PhD thesis. BI Norwegian School of Management.

Stephens, R. I., Burnham, K. J., and Reeve, P. J., 1995. A practical approach to the design of fuzzyy controllers with application to dynamic ship positioning. *Proceedings of IFAC Conference on Control Applications in Marine Systems*. Norway, Trondheim.

Strand, J. P., 1999. Nonlinear position control systems design for marine vessels. PhD thesis. Norwegian University of Science and Technology.

Tannuri, E. A., Agostinho, A. C., Morishita, H. M., and Moratelli Jr., I., 2010. Dynamic positioning systems: An experimental analysis of siliding mode control. *Control Engineering Practice*, **18** (10): 1121-1132.

Volovodov, S. K., Smolnikov, A. V., Volovodov, S. S., and Lampe, B. P., 2007. Synthesis of exponentially stable dynamic positioning systems for sea mobile objects using Lyapunov's method. *Proceedings of 12th Symposium Maritime Elektrotechnik*. Rostock, Germany.

Wu, L. Q., Lin, H., and Han, J. Q., 2004. Study of tracking differentiator on filtering. *Journal of System Simulation*, **16** (4): 651-670 (in Chinese).

Zheng, Q., and Gao, Z., 2010. On practical applications of active disturbance rejection control. *Proceedings of the 2010 Chinese Control Conference*, Beijing, 6095-6100.

Zhu, J., Zhang, Z., and Yang, H., 2006. An extended state observer based on tracking differentiator. *Proceedings of the 25th Chinese Control Conference.* Harbin, China, 85-88 (in Chinese).

(Edited by Xie Jun)